BIOCHEMISTRY
including biophysical chemistry & molecular biology

ARTICLE

pubs.acs.org/biochemistry

Binding Site for *Xenopus* Ribosomal Protein L5 and Accompanying Structural Changes in 5S rRNA

J. Benjamin Scripture and Paul W. Huber*

Department of Chemistry and Biochemistry, University of Notre Dame, Notre Dame, Indiana 46556, United States

Supporting Information

ABSTRACT: The structure of the eukaryotic L5−5S rRNA complex was investigated in protection and interference experiments and is compared with the corresponding structure (L18−5S rRNA) in the *Haloarcula marismortui* 50S subunit. In close correspondence with the archaeal structure, the contact sites for the eukaryotic ribosomal protein are located primarily in helix III and loop C and secondarily in loop A and helix V. While the former is unique to L5, the latter is also a critical contact site for transcription factor IIIA (TFIIIA), accounting for the mutually exclusive binding of these two proteins to 5S RNA. The binding of L5 causes structural changes in loops B and C that expose nucleotides that contact the *Xenopus* L11 ortholog in *H. marismortui*. This induced change in the structure of the RNA reveals the origins of the cooperative binding to 5S rRNA that has been observed for the bacterial counterparts of these proteins. The native structure of helix IV and loop D antagonizes binding of L5, indicating that this region of the RNA is dynamic and also influenced by the protein. Examination of the crystal structures of *Thermus thermophilus* ribosomes in the pre- and post-translocation states identified changes in loop D and in the surrounding region of 23S rRNA that support the proposal that 5S rRNA acts to transmit information between different functional domains of the large subunit.

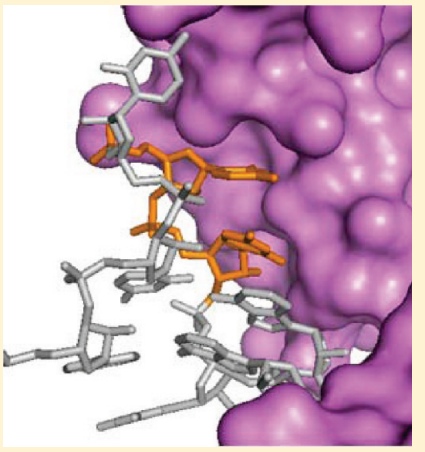

In eukaryotes, there is an extraribosomal pool of 5S rRNA associated with ribosomal protein L5.[1,2] The functional significance of this RNP complex is not entirely clear, but most likely L5 is acting as a chaperone to deliver the RNA to the site of ribosome assembly. The 5S rRNA genes, which are transcribed by RNA polymerase III, are not associated with other rRNA genes, which are transcribed by RNA polymerase I in the nucleolus. Pulse−chase experiments in HeLa cells provided evidence that the L5−5S rRNA complex is ultimately incorporated into ribosomes.[2] Yeast also has a measurable amount of the L5−5S rRNA complex,[1] and recent experiments have determined that assembly factors Rpf2 and Rrs1 are necessary for recruiting L5, 5S rRNA, and ribosomal protein L11 into 90S preribosomal particles.[3]

The metabolism of 5S rRNA in amphibian (*Xenopus*) oocytes is more complex, because the synthesis of L5 and 5S rRNA is asynchronous.[4] Approximately 100,000 copies of 5S rRNA genes are actively transcribed during the early stages of oogenesis; however, expression of L5 does not begin until vitellogenesis at the midstage of oogenesis. As a result, 5S rRNA is stored in two cytoplasmic RNP complexes for several weeks until it is mobilized for ribosome biogenesis. The stored 5S rRNA is bound to either the zinc finger protein, transcription factor IIIA (TFIIIA), or a related protein, p43/thesaurin-b.[5−8] In the latter instance, the p43−5S rRNA complex is part of a larger 42S structure that also contains thesaurin-a and tRNA.[8]

The accumulated cytoplasmic 5S rRNA is somehow transferred to L5, which is required for transport of this RNA into the nucleus.[9−14] Various protection and mutagenesis experiments have been used to define the binding sites for TFIIIA[15−29] and L5[30−35] on 5S rRNA. Both binding sites encompass large segments of the RNA, indicating that interaction of the proteins with 5S rRNA is mutually exclusive. Biochemical experiments indicated that the N-terminus of TFIIIA is proximal to loop D and the protein appears to extend linearly through helix IV, loop E, helix V, loop A, helix II, and loop B, ending with its C-terminus positioned in the vicinity of helix III and loop C.[19] This orientation of the protein has been confirmed in two high-resolution structures of fragments of TFIIIA bound to truncated versions of 5S rRNA. Crystal[36] and NMR[37] structures of zinc fingers 4−6 bound to the central region of 5S rRNA show that finger 4 is positioned at loop E, finger 5 at helix V, and finger 6 at loop A.

The α-sarcin footprint of rat L5 on 5S rRNA extends over much of the same region as that for TFIIIA;[18,32] however, subsequent mutagenesis experiments revealed that nucleotides in the helix III−loop C hairpin are the major determinants of binding of L5 to 5S rRNA.[35] Indeed, a direct comparison of the effects of a family of mutations in 5S rRNA on the binding of TFIIIA and L5 exhibited few notable similarities between the two.[35] Thus, despite largely overlapping binding sites defined by enzymatic footprinting, TFIIIA and L5 appear to utilize different subsets of these sites as critical identity elements.

Received: February 24, 2011
Revised: March 28, 2011
Published: March 29, 2011

In previous experiments, we used chemical nucleases in protection and interference assays to characterize the interaction of TFIIIA with 5S rRNA.[29] The smaller size of these cleavage reagents minimizes the effects of steric hindrance that complicate the interpretation of protection experiments using protein nucleases.[38] Notably, "missing nucleoside" experiments indicated that the loop E−helix V region is a major determinant for binding of TFIIIA,[29] which was later confirmed by the crystal and NMR structures. Here we have applied these techniques to an analysis of the *Xenopus* L5−5S rRNA complex. The results verify that helix III and positions in loop C are critical for binding of L5 and reveal other sites of close association between the protein and RNA located in loop A and helix V. In addition, the data provide evidence of L5-induced changes in the structure of loops B and C that create contact sites for ribosomal protein L11. The missing nucleoside experiments reveal that the native loop D−helix IV structure adversely affects binding of L5 to 5S rRNA, indicating the protein may influence the dynamics of this domain of the RNA. This observation prompted us to examine the crystal structures of ribosomes at various stages of the protein synthesis cycle. We have found that there are differences in the structure of loop D and its interaction with 23S rRNA between pre- and post-translocation ribosomes that are consistent with proposals that 5S rRNA transmits signals between functional sites within the ribosome.[39−43]

EXPERIMENTAL PROCEDURES

Several of the experimental procedures have been described previously, including the preparation of native 5S rRNA, synthesis of RNA by runoff transcription, and the radiolabeling of RNA;[20] expression and purification of L5 as a fusion with maltose binding protein (fL5); and 5S rRNA binding assays.[35]

α-Sarcin Footprinting. After digestion of fL5 with factor Xa to remove the MBP domain, L5 (100 nM) was incubated with 5′- or 3′-end radiolabeled 5S rRNA as previously described.[35] The indicated amount of α-sarcin was added, and samples were incubated at 30 °C for 5 min. Digestions were stopped by the addition of 1 μg of tRNA and sodium acetate to a concentration of 0.3 M, followed by extraction with phenol and chloroform and precipitation with ethanol. The samples were analyzed on sequencing gels (10 or 20%) alongside RNase T1 and alkaline hydrolysates of 5S rRNA.

Hydroxyl Radical Footprinting. Because the L5 binding buffer contains glycerol, which is a strong scavenger of hydroxyl radicals, the L5−5S rRNA complex was exchanged into binding buffer lacking glycerol by being passed through a spin column (Ambion). Cleavage reactions were conducted essentially as described previously.[29] Reaction volumes generally were 20 μL and contained (final concentrations) 100 μM iron(II), 200 μM EDTA, 0.015% hydrogen peroxide, and 1 mM ascorbate. Reactions proceeded for 2 min at 28 °C and were quenched with 10 mM thiourea and 2 mM EDTA. The RNA was precipitated with ethanol using 1−2 μg of tRNA as carrier, and the pellets were washed multiple times with 70% ethanol to remove residual $Fe[EDTA]^{2-}$. The samples were analyzed on sequencing gels.

Missing Nucleoside Experiments. Renatured 5S rRNA was cleaved with $Fe[EDTA]^{2-}$ and H_2O_2 and recovered by precipitation with ethanol. This procedure results in the loss of small fragments (8−10 nucleotides) from the 5′- and 3′-ends of the RNA. The gapped RNA was incubated with fL5 (an empirically determined amount that binds approximately half of the RNA) in binding buffer for 90 min at room temperature. Free 5S rRNA and bound 5S rRNA were separated by electrophoresis on 8% nondenaturing polyacrylamide gels.[29] These samples were then analyzed on sequencing gels, and autoradiographs were scanned with a laser densitometer (Molecular Dynamics) to quantitate differences between nucleotide positions in the free and bound fractions of the RNA.

Footprinting with Phosphorothioate Nucleotides. Synthesis of 5S rRNA containing 5′-*O*-(1-thio)nucleotides was modified from the standard procedure.[20] The concentration of phosphorothioate nucleoside triphosphate (Glen Research) was 350 μM, and the concentration of the standard ribonucleotides was reduced to 1.4 mM. Binding reactions with L5 were as described above. Samples were placed on ice for cleavage with iodine (150 μM in ethanol) for 30 s; the reactions were stopped by extraction with phenol.[44]

CONTACT/ACT Analysis. Predicted intersubunit contacts between *Haloarcula marismortui* L18 and 5S rRNA were calculated using CONTACT/ACT with atom to atom search limits of 2.0−3.5 Å.[45] All structural illustrations were prepared with PyMOL (DeLano Scientific LLC, San Carlos, CA).

RESULTS

α-Sarcin Footprint of *Xenopus* L5 on 5S rRNA. α-Sarcin is a cytotoxic ribonuclease that inactivates ribosomes by precise cleavage of a conserved site, the sarcin−ricin domain, in the large rRNA.[46] At high concentrations, it is a purine-specific ribonuclease that is largely insensitive to secondary structure.[47] Thus, α-sarcin can generate digestion ladders sufficient for footprinting the binding sites of proteins on RNA.[48] In earlier experiments, the eukaryotic L5−5S rRNA complex was released from rat ribosomes by treatment with EDTA and end-labeled [^{32}P]5S rRNA allowed to exchange into the complex. The region of 5S rRNA protected from α-sarcin digestion was extensive and included all but the loop B−helix III−loop C region.[32] However, later experiments that aimed to characterize the binding of *Xenopus* L5 to mutant variants of 5S rRNA indicated that critical nucleotides were limited to the helix III−loop C hairpin.[35] Because there is little difference in the sequences of the rat and *Xenopus* proteins and RNAs, the disparity seemed artifactual rather than reflecting true differences in the structures of the complexes. It seemed more likely that the methods used to form the *Xenopus* L5−5S rRNA complexes, prepared by direct reconstitution using purified protein and RNA, could account for the discrepancy.

Figure 1 shows the α-sarcin footprint of the *Xenopus* L5−5S rRNA complex. A considerable amount of the RNA is protected from digestion; the only exposed region is located in loop D (nucleotides 83−89). Thus, under these conditions, the footprint includes not only the region identified previously but also the helix III−loop C domain identified in mutagenesis experiments. This result may indicate that the ability of 5S rRNA to exchange into the L5−5S rRNA complex by incubation in EDTA is due to a disruption of contacts between the protein and its critical identity elements in metal-free medium; optimal binding of L5 to 5S rRNA occurs in 0.5 mM magnesium.[35] Notwithstanding this point, the important observation in this case is that, in the reconstituted RNP complex, the protein does protect nucleotides identified by mutagenesis from digestion with α-sarcin. Moreover, a large amount of the RNA molecule is resistant to ribonuclease digestion when bound to L5, which ostensibly reflects the ability of this RNP complex to exist independently of the ribosome in vivo.

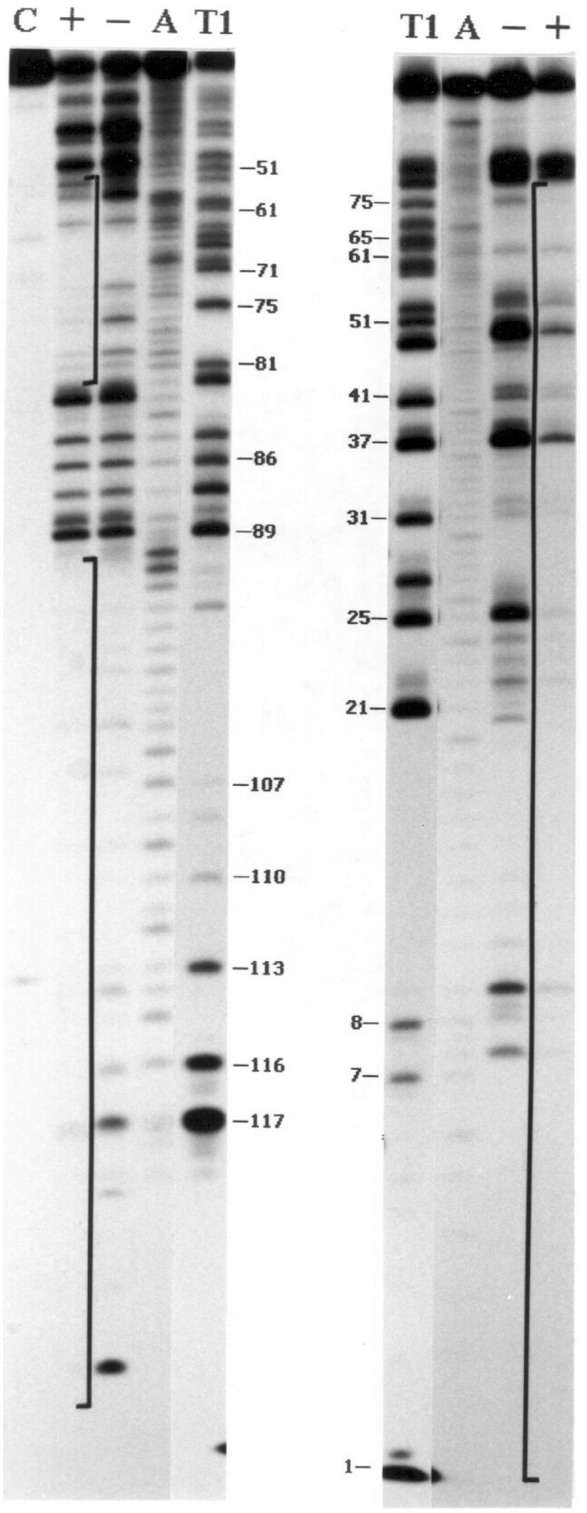

Figure 1. α-Sarcin protection analysis of the L5−5S rRNA complex. 5S rRNA (~2 nM) radiolabeled at the 3′-end (left) or 5′-end (right) was incubated without (−) or with (+) 100 nM L5. Samples were digested for 5 min with 5 μM α-sarcin. Digests were analyzed alongside ribonuclease (T1) and alkaline (A) digests and undigested control RNA (C) on denaturing polyacrylamide gels. Brackets enclose regions of protection.

Hydroxyl Radical Footprint of *Xenopus* L5 on 5S rRNA. The protection pattern observed with α-sarcin establishes that a considerable amount of 5S rRNA can be protected from ribonuclease digestion by L5; however, it reveals little about contact sites on the RNA. Hydroxyl radicals cleave nucleic acids in a sequence-neutral fashion. Moreover, because of its small size, this reagent essentially probes the solvent accessible surface of a nucleic acid, providing a high-resolution picture of a protein−nucleic acid complex.[38,49] As expected, the regions with diminished cleavage by hydroxyl radicals in the presence of L5 are a subset of the α-sarcin footprint (Figure 2). The protected region extends from helix I through loop A, helix II, loop B, helix III, and the proximal region of loop C (Figure 3). It is noteworthy that the strongest protection occurs in helix III and the base of loop C, fully consistent with the results from mutagenesis.

Iodoethane Footprint of *Xenopus* L5 on 5S rRNA. Hydroxyl radicals react with hydrogens on the ribose ring, preferably at the 5′ and 4′ positions, which leads to strand scission.[50] Protection from this reagent provides information about regions of close association between the protein and the RNA backbone. Alkylation of 5′-*O*-(1-thio)nucleotides by iodoethane leads to spontaneous hydrolysis;[51] thus, this reagent can also be used to probe protection of the backbone, but at the position of the phosphate rather than the ribose. Samples of 5S rRNA were prepared that, individually, had one of the four 5′-*O*-(1-thio)nucleotides randomly incorporated by runoff transcription. Complexes of L5 bound to the modified RNAs were treated with iodoethane and compared to digests of free RNA (Figure 4).

The RNA in the complex exhibited sites of protection and sites of enhanced cleavage, both of which are found within the hydroxyl radical footprint (Figure 3), indicating good concordance between the two probes. Protected sites are clustered in helix III and at the junction with loop C, providing more evidence that this is the critical site of interaction between L5 and 5S rRNA. The small region at the top of loop C that is exposed in the hydroxyl radical footprint contains two nucleotides (U_{40} and G_{41}) that exhibit enhanced cleavage by iodoethane in the RNP complex. Interestingly, the converse situation occurs in the region of loop B between nucleotides 54 and 58. There is clear protection of this region in the hydroxyl radical footprint, yet A_{54}, U_{55}, and A_{58} are more reactive with iodoethane in the presence of L5. On the opposite strand there is both protection (A_{22}, A_{23}, A_{24}, and U_{26}) and enhancement (G_{25}). *Xenopus* L5 binds to 5S rRNA through a mutual induced fit mechanism.[52] The mixed increased/decreased cutting by iodoethane in the region of loop B and loop C locates at least some of these protein-dependent structural changes in 5S rRNA.

Missing Nucleoside Experiment. In this experiment, hydroxyl radicals are used to introduce single-nucleoside gaps randomly throughout the nucleic acid.[29,38,53] The damaged nucleic acid is incubated with its cognate binding protein, and then free and bound nucleic acids are separated and analyzed by electrophoresis on sequencing gels. Fragments enriched in the unbound fraction represent positions at which the missing nucleoside interfered with binding of the protein. In the case of DNA, with its regular double-helical structure, interpretation of the data is straightforward; however, because of its extensive secondary and tertiary structure, RNA experiments are more complex. An important caveat is that a missing nucleoside may perturb the structure of the RNA, which then has an indirect, secondary effect on protein binding. An associated problem, noted earlier, is that recovery of some fragments is poor, and these positions are underrepresented on the subsequent sequencing gel.[29,38] Notwithstanding these complications, this technique was used

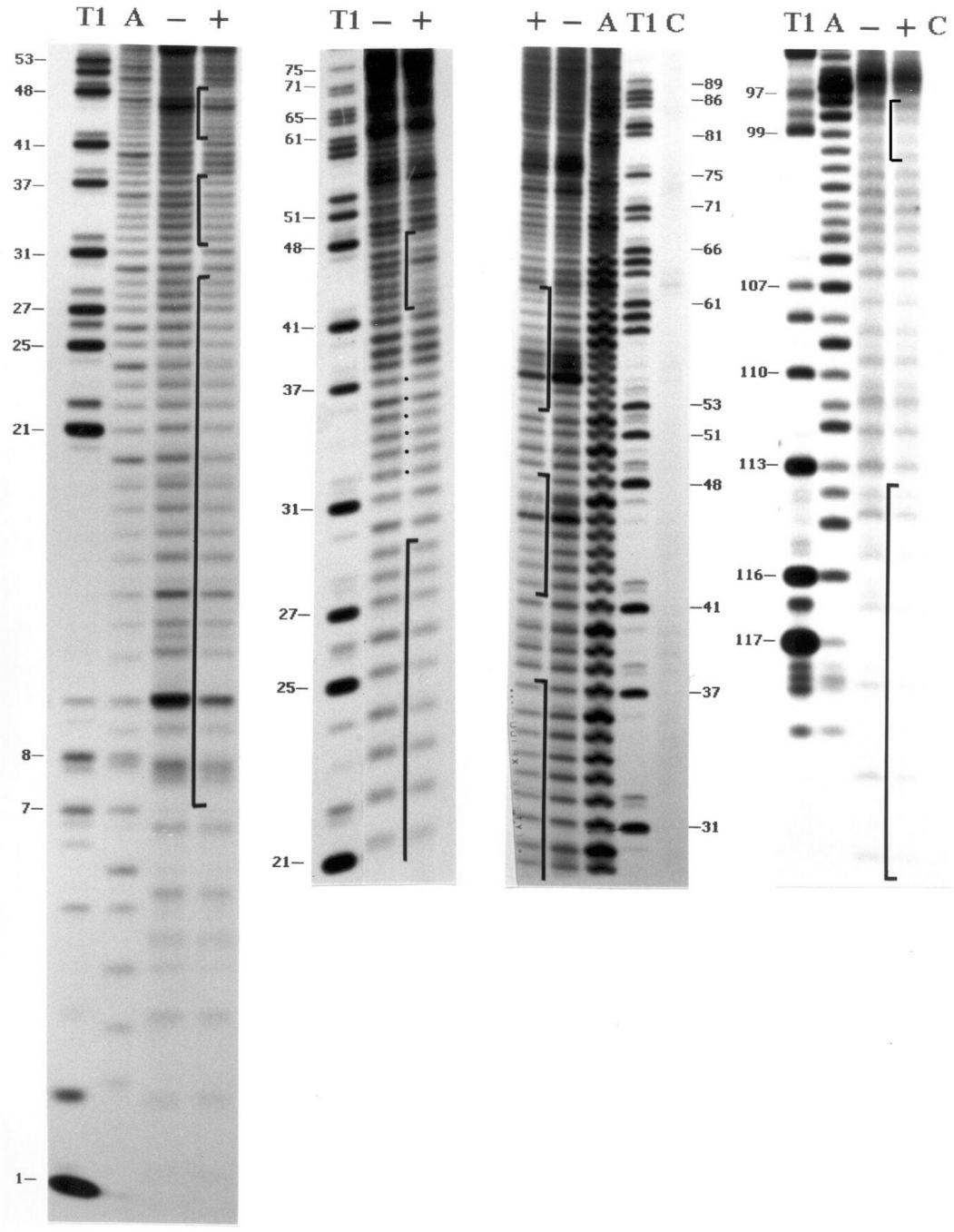

Figure 2. Hydroxyl radical analysis of the L5−5S rRNA complex. The complex was formed under standard conditions with 3′- or 5′-end-labeled 5S rRNA and then passed through a spin column to remove glycerol. Cleavage reactions of 5S rRNA (−) and the L5−5S rRNA complex (+) were analyzed alongside ribonuclease (T1) and alkaline (A) digests and undigested control RNA (C) on denaturing polyacrylamide gels. Brackets enclose regions of protection.

successfully to identify loop E and helix V as key recognition elements for TFIIIA.[29]

End-labeled 5S rRNA was gapped using $Fe[EDTA]^{2-}$ and H_2O_2 and then incubated under standard conditions with L5. Bound 5S rRNA and free 5S rRNA were separated on a nondenaturing polyacrylamide gel and isolated for subsequent analysis on sequencing gels (Figure 5). During this process, small RNA fragments are lost; thus, helix I cannot be tested by this method. Similar to the footprinting experiment with iodoethane, there were positions at which a missing nucleoside interfered with binding of L5 or, alternatively, enhanced binding. To improve the visualization of the difference between the bound and free samples, the autoradiographs were scanned with a laser densitometer (Figure 6). The most deleterious effects of gapping the RNA occur between nucleotides 44 and 51 in helix III. On the opposite side of helix III, missing nucleotides at positions 27−30 interfere with binding, as do U_{35} and C_{36} in loop C. In loop A, U_{109} shows particularly strong interference; this position is also protected from iodoethane. Indeed, there is remarkably good overall agreement between the iodoethane footprinting data and the missing nucleoside data (Figure 3).

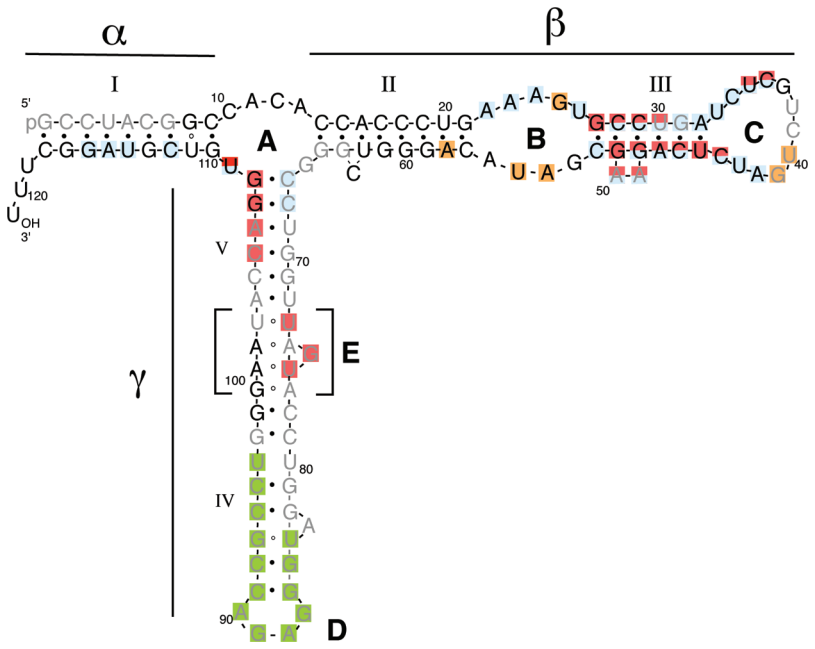

Figure 3. Secondary structure of *Xenopus* 5S rRNA with designations of the sites of protection or interference. Nucleotides protected by L5 from cleavage by hydroxyl radicals are colored black; exposed residues are colored gray. Phosphorothioate nucleotides that exhibit decreased (blue) or enhanced (orange) reaction with iodoethane or nucleotides enriched in the free (red) or bound (green) fractions of gapped (missing nucleoside) 5S rRNA are highlighted.

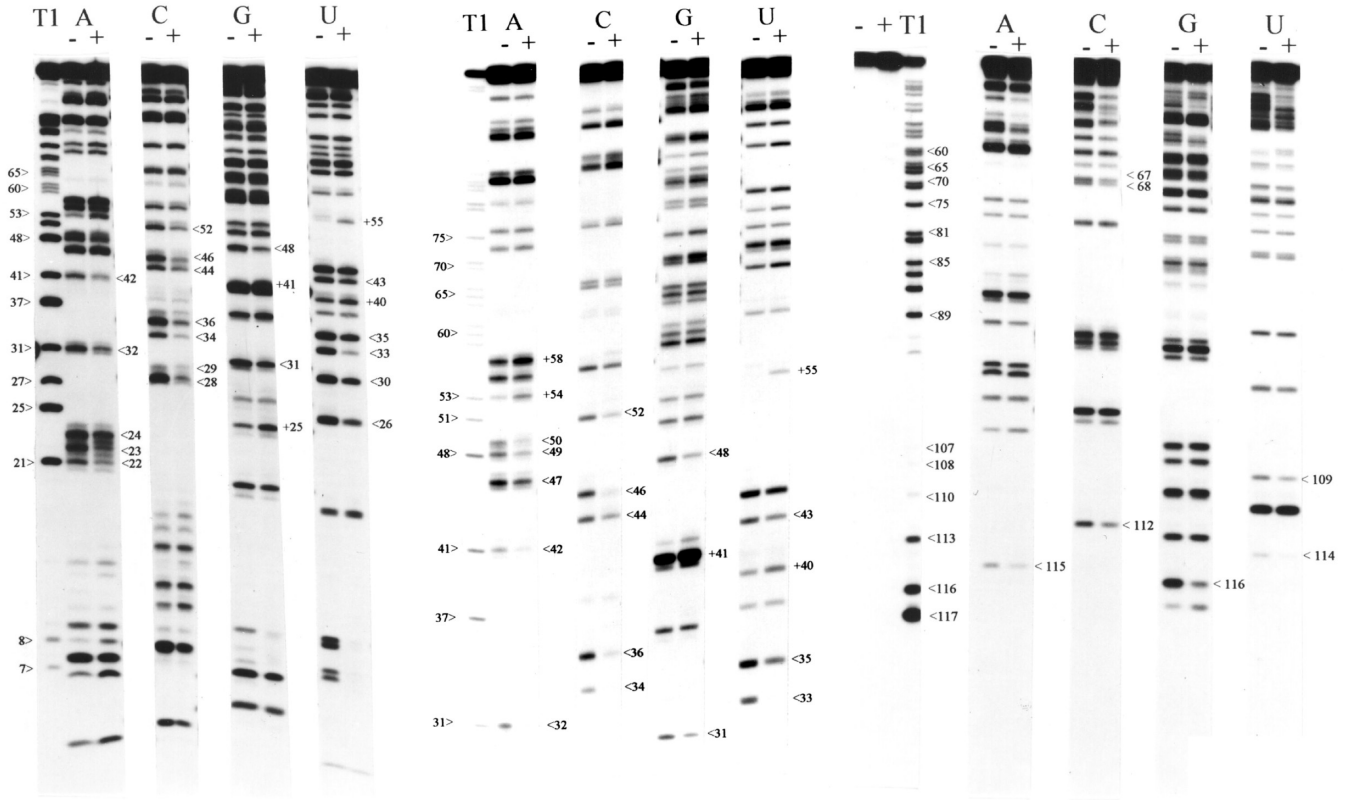

Figure 4. Iodoethane analysis of the L5−5S rRNA complex. 5S rRNA samples containing randomly incorporated phosphorothioate nucleotides were individually synthesized by runoff transcription. Free (−) and bound (+) RNA was treated with iodoethane to induce hydrolysis at the sites of the modified nucleotides and analyzed alongside a ribonuclease T1 digest of unmodified 5S rRNA. Note that the phosphorothioate nucleotides alter the migration of RNA fragments relative to the unmodified RNA; thus, the two do not comigrate exactly during electrophoresis. The phosphorothioate nucleotide is indicated at the top of each panel. Unmodified 5S rRNA with (+) or without (−) treatment with iodoethane is also shown. Nucleotide positions that exhibit decreased (<) or increased (+) cleavage in the presence of L5 are indicated on the right side of each panel.

dx.doi.org/10.1021/bi200286e |*Biochemistry* 2011, 50, 3827–3839

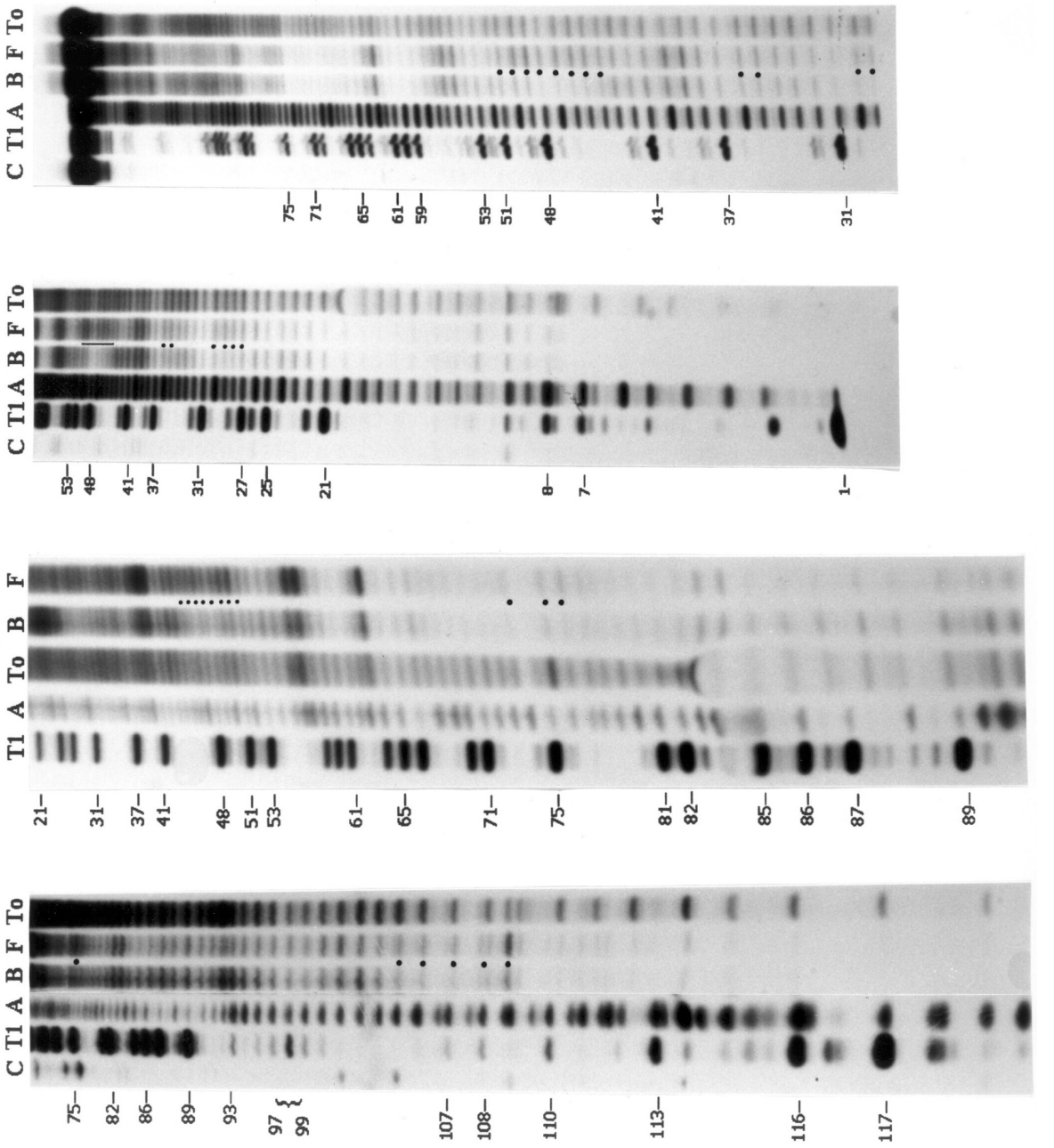

Figure 5. Missing nucleoside experiment. 5S rRNA radiolabeled at the 5′- or 3′-end was gapped using $Fe[EDTA]^{2-}$ and H_2O_2. The damaged RNA was incubated with L5, and bound and free RNA isolated after separation on a nondenaturing polyacrylamide gel. The RNA in bound (B) and free (F) fractions was compared by electrophoresis on denaturing gels alongside lanes containing untreated control RNA (C), gapped RNA prior to incubation with L5 (To), ribonuclease T1 (T1), and alkaline (A) digests. Filled circles and a bar indicate positions enriched in the population of free RNA.

There is a segment of 5S rRNA, extending from position 84 to 96, in which a missing nucleoside favors binding of L5. This region does not appear to be part of the contact site for L5. No protection from hydroxyl radicals or iodoethane is seen here, and various site-specific mutations at residues 83, 86, and 96 had no effect on the binding affinity for L5.[35] We speculate that gaps in this region, which includes loop D and part of helix IV, have an indirect effect that relieves a conformational constraint that normally has an adverse effect on binding of L5. Mirroring this effect, a quadruple (G → C) mutation at positions 70, 71, 81, and 82, which weakens the helices flanking loop E, binds to L5 with a slightly higher affinity than wild-type 5S rRNA.[35] It is clear from the missing nucleoside experiment and the earlier mutagenesis experiments that, in solution, this region of 5S rRNA (loop E−helix IV−loop D) may be in a conformation that confers some energetic penalty upon binding L5. It is unlikely that eukaryotic L5 makes substantive contact with this arm of the molecule. Although the α-sarcin footprint includes loop E and much of helix IV, the smaller footprinting reagents did not reveal any protection beyond the junction of helix V with loop A.

DISCUSSION

Comparison to the *H. marismortui* L18−5S rRNA Complex. The results of these protection and interference experiments will be

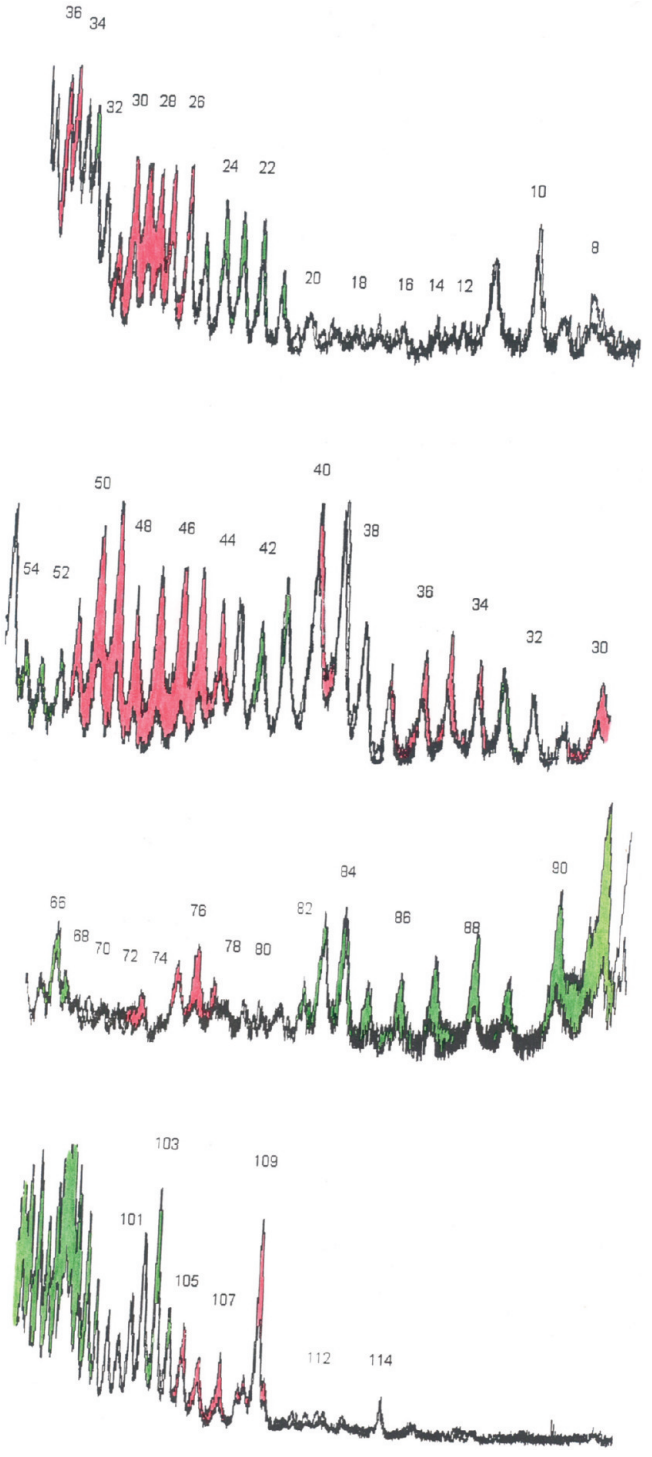

Figure 6. Densitometric analysis of the missing nucleoside experiment. The lanes in the autoradiograph containing free and bound fractions of RNA were scanned with a laser densitometer for comparison of the relative intensity at each nucleotide position. The differences show positions enriched in the free (red) or bound (green) fractions. The positions of even-numbered nucleotides are given.

discussed relative to the structure of the 50S subunit of *H. marismortui*, because the crystal (4.1 Å) and electron cryomicroscopy (8.7 Å) structures of eukaryotic ribosomes remain below the resolution of the archaeal structure.[54,55] The *H. marismortui* homologue of

Table 1. Homologous Ribosomal Proteins

eukaryote	archaea	eubacteria
L5	L18	L18
L11	L5	L5

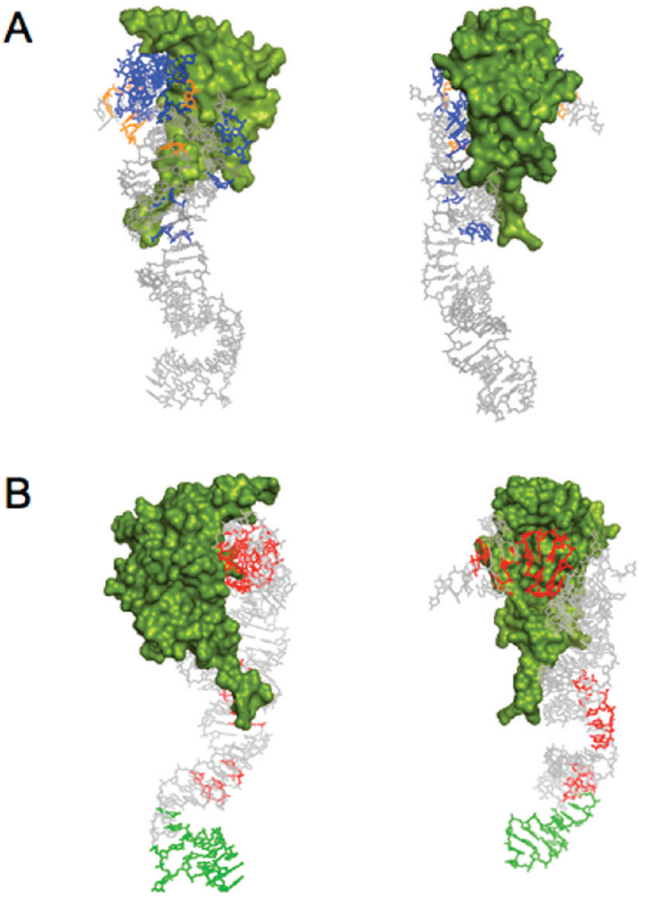

Figure 7. Map of sites of protection or interference on the crystal structure of *H. marismortui* 5S rRNA. (A) Two views of the 5S rRNA−L18 complex. Phosphorothioate nucleotides that exhibited reduced (blue) or enhanced (orange) cleavage by iodoethane are indicated along with a surface representation of L18. (B) Nucleotide positions that were enriched in the free (red) or bound (green) fractions in the missing nucleotide experiments are indicated. The coloring is the same as in Figure 3.

L5 is L18 (Table 1). These proteins are 35% identical and differ considerably in length, 296 versus 186 amino acids. Approximately half of this difference in size is accounted for by an extension of the C-terminal end of L5, deletion of which severely weakens binding to 5S rRNA.[10] While this effect might suggest the possibility of interactions between this segment of L5 and 5S rRNA, the C-terminus of the archaeal protein is distal to the RNA, so it is not obvious how the eukaryotic protein contributes additional contacts to the RNA. Nonetheless, a region of protection on *Xenopus* 5S rRNA not identified in the *H. marismortui* structure must be considered a potential contact site for the C-terminal end of L5.

The nucleotides identified in the iodoethane protection (Figure 7A) and missing nucleoside (Figure 7B) experiments are highlighted on the structure of the *H. marismortui* L18−5S rRNA complex. There is a good correspondence between the

positions identified in these experiments and their location relative to L18 in the archaeal structure, suggesting that any potential interactions between the C-terminus of L5 and the RNA are limited. A deep trough in L18 makes close contact with helix III and the base of loop C that can account for much of the protection pattern seen with the *Xenopus* protein. The top of loop C protrudes from the surface of *H. marismortui* L18, consistent with the absence of any protection in the eukaryotic complex. The ribose−phosphate backbone at the 3′-end of the archaeal RNA is buried in the protein, accounting for the protection we detect at *Xenopus* residues 114−116.[a]

The N-terminus of *H. marismortui* L18 is an extended segment that makes contact with the three-way helical junction at loop A. The C_{10}ACA sequence, common to archaeal and eukaryotic 5S rRNAs, makes a considerable number of contacts with *H. marismortui* L18, and we observe protection of these nucleotides from hydroxyl radicals by L5. However, there was no detectable protection from iodoethane. In the archaeal structure, most of the protein contacts are to the bases, with the backbone in this segment exposed, accounting for the phosphorothioate linkages that are susceptible to alkylation and cleavage in the *Xenopus* complex. Hydroxyl radicals target ribose positions (C4′ and C5′) in the minor groove,[50] which explains the difference between probing with $Fe[EDTA]^{2-}$ and H_2O_2 and probing with iodoethane and is consistent with L5 also making contact with the bases at these positions in loop A.

Overlapping Sites for L5 and TFIIIA on 5S rRNA. In atomic-resolution structures, the loop A junction makes a variety of contacts with TFIIIA and *H. marismortui* L18. Interestingly, the structure of the loop, which is conformationally heterogeneous in the absence of protein, is quite similar in the two complexes despite entirely different interactions with the two disparate proteins.[36,37,56,57] The N-terminus of eukaryotic L5 contains a nine-amino acid extension compared with the archaeal ribosomal protein, and this extra segment appears to run from loop A to helix V. Protection by L5 from hydroxyl radicals occurs at residues 107−109 and from iodoethane at residues 67 and 68; however, the corresponding nucleotides in *H. marismortui* 5S rRNA do not contact L18. In the missing nucleoside experiments, five positions in helix V extending into the junction with loop A exhibit diminished binding, supporting the results of the protection assays. The phosphates at C_{67} and C_{68} protected by L5 from iodoethane are particularly noteworthy, because they also make hydrogen bond contacts with zinc finger 5 of TFIIIA.[36] Much of the free energy of binding of TFIIIA to 5S rRNA comes from contacts made by zinc fingers 5 and 6 to helix V and loop A, respectively;[19,36,37,58,59] consequently, this region of the RNA is likely the major arbiter of the mutually exclusive binding of the two proteins. Hence, the small N-terminal extension of eukaryotic L5 is especially significant in this regard, because it contributes to the competition for common contact sites in the RNA.

L5-Dependent Changes in the Structure of Loops B and C and Contacts with L11. The loop B region exhibits sites of reduced and enhanced cleavage by iodoethane. The basis for the observed protection is not obvious from the archaeal crystal structure, because this segment appears pushed away from L18; possibly, this is a site of contact with the C-terminal extension in eukaryotic L5. The nucleotides that exhibit increased reactivity with iodoethane, however, show a remarkable relationship with archaeal ribosomal protein L5 that also contacts 5S rRNA. Figure 8 shows that four of the six nucleotides in loop B and loop C that exhibited enhanced cleavage, in fact, contact *H. marismortui* L5. *Xenopus*

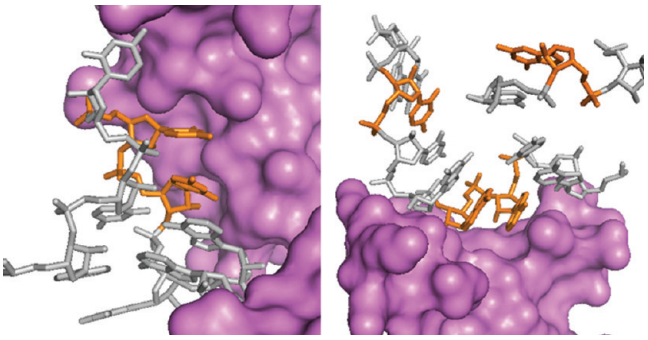

Figure 8. Sites of enhanced cleavage by iodoethane relative to *H. marismortui* L5. Nucleotides that exhibited enhanced cleavage by iodoethane (orange) are shown relative to a surface representation of *H. marismortui* L5, the homologue of eukaryotic L11, which also makes contact with 5S rRNA: nucleotides 40 and 41 in loop C at the left and nucleotides 25, 54, 55, and 58 in loop B at the right.

ribosomal protein L11 is the homologue of archaeal L5 (Table 1), and the former is similarly positioned adjacent to 5S rRNA in the cryo-EM structures of yeast[60] and mammalian[55] ribosomes. This indicates that a conformational change engendered by the binding of *Xenopus* L5 exposes nucleotides in 5S rRNA required for interactions with L11. *Xenopus* L5 alters the CD spectrum of 5S rRNA, providing direct evidence of a protein-induced change in the RNA structure.[52] This scenario parallels that for the *Escherichia coli* homologues of these two proteins (Table 1). *E. coli* L18 (*Xenopus* L5), which also changes the CD spectrum of 5S rRNA, has a cooperative influence on the binding of *E. coli* L5 (*Xenopus* L11), increasing the binding affinity of the latter by roughly 1 order of magnitude.[61,62] The molecular basis for this cooperative mechanism can now be understood in terms of the induced fit binding of one ribosomal protein (*Xenopus* L5 or *E. coli* L18) that then creates a specific binding site for a second protein (*Xenopus* L11 or *E. coli* L5).

This induced change in the structure of 5S rRNA may play a role in ribosome assembly. The incorporation of the L5−5S rRNA complex into 90S preribosomal particles appears to take place within the context of a larger complex that contains ribosomal protein L11 and two assembly factors, Rpf2 and Rrs1.[3] The L5-induced structural change in 5S rRNA seemingly allows or facilitates the latter's interaction with L11 and may serve as a quality control mechanism, because the complete RNP particle is required for integration into preribosomes.[3]

The γ-Domain and the Function of 5S rRNA. The γ-domain of 5S RNA includes loop D, helix IV, loop E, and helix V.[63] Three missing nucleosides in loop E, including two (G_{75} and U_{76}) that comprise the base triple that defines the structure of the loop, have a modest effect on L5 despite being well outside the contact region of the archaeal protein and not exhibiting any protection from hydroxyl radicals or iodoethane (Figure 3). Mutagenesis experiments demonstrate that disruptions in loop E can cause global changes in the structure of 5S rRNA, accounting for the effect of missing nucleotides at these positions.[35] Four nucleotides (98−101) on the opposite strand of loop E exhibit diminished cleavage by hydroxyl radicals when L5 is bound, which we believe is caused by a structural change in the RNA rather than protection by the protein, because none of these positions is protected from iodoethane. Solvent accessibility influences the degree of cleavage by hydroxyl radicals and is, in fact, used to map RNA tertiary structure and folding (reviewed by Tullius and Greenbaum in ref 64). It is noteworthy that A_{100} and

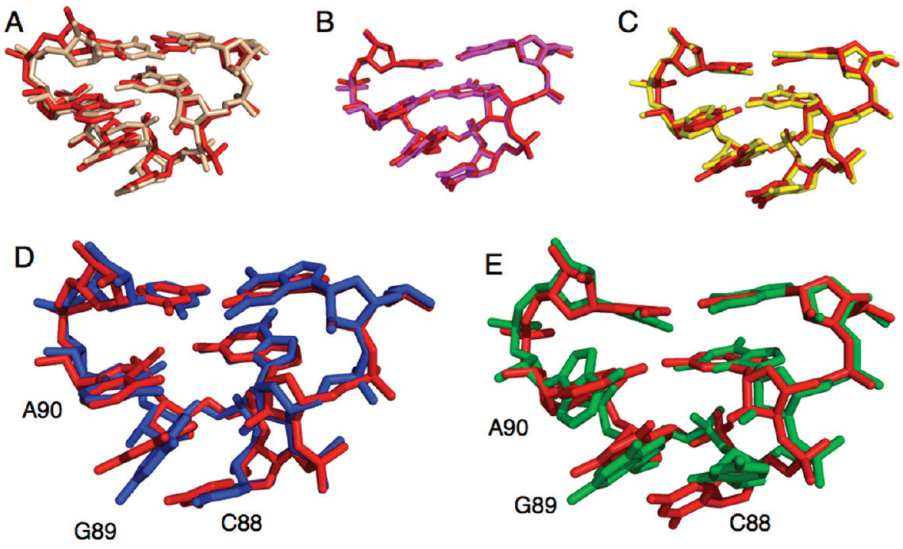

Figure 9. Comparison of the structures of loop D. The *T. thermophilus* ribosome with all three tRNA binding sites occupied (red, PDB entry 2J01) is taken as the reference structure and is compared with (A) *H. marismortui* (pink, PDB entry 1S72), (B) *T. thermophilus* prepeptidyl transfer (magenta, PDB entry 2WDN), (C) *T. thermophilus* postpeptidyl transfer (yellow, PDB entry 2WDJ), (D) *T. thermophilus* ternary complex with bound EF-Tu and aminoacyl-tRNA (blue, PDB entry 2WRR), and (E) *T. thermophilus* with bound EF-G−GDP and fusidic acid (green, PDB entry 2WRJ).

A_{101} are part of an A-minor motif that contacts helix 38 in 23S rRNA that contains the A-site finger (ASF) that helps position tRNA in the A-site.[65,66] Mutations that shorten the ASF affect translocation and enhance frameshift activity,[67] which echoes the effects of mutations in either yeast L5 or 5S rRNA.[41,43,68]

Missing nucleosides in portions of helix IV and loop D enhance binding of L5 (Figures 3 and 7B). This region exhibited no protection from α-sarcin, hydroxyl radicals, or iodoethane, suggesting that the inherent structure of this region of 5S rRNA confers an energetic penalty on the binding of L5. This result is consistent with the modestly increased binding affinity of L5 for a quadruple mutant that disrupts G·C base pairs in helices IV and V and, presumably, destabilizes this region of the RNA.[35] Long-range structural changes involving this arm of 5S rRNA are particularly significant given the biochemical evidence that this region makes direct and indirect contacts with functionally important sites in the large rRNA. In *E. coli* ribosomes, U_{89} in loop D can be cross-linked to sites near the peptidyl transferase center (PTC) and the GTPase-associated center (GAC) in 23S rRNA.[39,40] Similarly, mutations at a conserved nucleotide (A_{960}) of the GAC trigger structural changes at loop D and the PTC.[42] These observations have led to the proposal that 5S rRNA, and more specifically loop D, acts to transmit signals between these two active centers of the ribosome. In saturation mutagenesis studies of yeast 5S rRNA, the resulting phenotypes were assigned to mutations that clustered in three regions: loop B and helix III, which can be ascribed to interactions with L5 and L11 and contacts with the small subunit; loop E, ascribed to effects on the A-site finger; and helix IV and loop D, ascribed to direct and indirect contacts with the PTC, GAC, and sarcin−ricin domain.[41,43] These studies provide genetic evidence that functional domains of the ribosome might coordinate their activity through 5S rRNA acting as a sort of relay center.

The structural probing experiments reported here not only provide evidence of conformational flexibility in the γ-domain that supports this model but also indicate that L5 may modulate these structural transitions. Consequently, we asked whether there are any appreciable changes in the structure of 5S rRNA, specifically in the γ-domain and the surrounding regions of 23S rRNA, that can be seen in any of the high-resolution crystal structures of ribosomes at various stages of the protein synthesis cycle. We have focused on the *T. thermophilus* ribosome for this analysis, because there are several atomic-resolution structures presently available that allow for comparisons without the complication of sequence and phylogenetic structural differences. We have identified changes in the local structures of loops E and D. Those in loop E will not be addressed here, because the secondary structure of this region differs between bacterial and eukaryotic 5S rRNA and changes in the former cannot be easily correlated with the protection−interference data reported here for *Xenopus* 5S rRNA. Nonetheless, these changes do suggest that the structure of loop E is dynamic, and a full analysis of the loop E structures will be reported separately.

The structures of loop D are all compared to that of a pretranslocation *T. thermophilus* ribosome bound to mRNA with all three tRNA sites (A, P, and E) occupied [Protein Data Bank (PDB) entry 2J01].[69] Notably, the loop D nucleotides of *T. thermophilus* and *H. marismortui*, which have identical sequences, align well (rmsd of 0.62), indicating that the structure of the loop is likely comparable across all three kingdoms (Figure 9A). This comparison between the archaeal and bacterial loops also provides some sense of what changes in the series of *T. thermophilus* structures may be significant. Loop D in *T. thermophilus* ribosomes representing the pre- and postpeptidyl transfer states (Figure 9B,C) superimposes on the reference structure (rmsd values of 0.59 and 0.39, respectively) with no notable differences.[70] The structure of the 70S ribosome bound to the ternary complex of aminoacyl-tRNA−EF-Tu−GDP (Figure 9D) does exhibit some change in the orientation of the base of G_{89} that is reflected in a small increase in the rmsd (0.70).[71] However, the *T. thermophilus* ribosome bound to the EF-G−GDP complex and locked in the post-translocation state with fusidic acid (Figure 9E) has marked changes in the structure of loop D (rmsd of 0.90). A roughly 60° rotation around the glycosidic

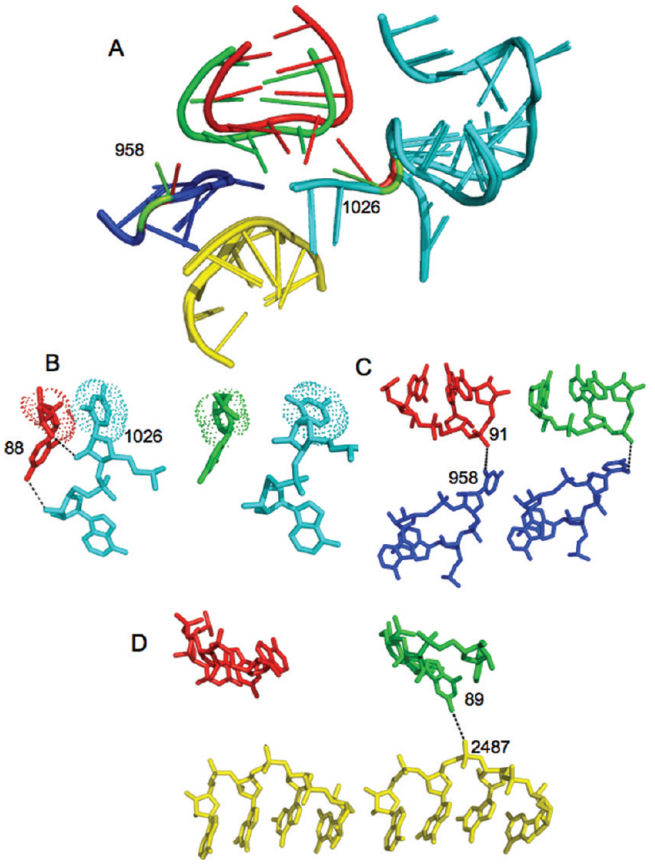

Figure 10. Comparison of pre- and post-translocation ribosomes. Loop D residues of the pre-translocation ribosome (PDB entry 2J01) are colored red and those of the post-translocation ribosome (PDB entry 2WRJ) green. (A) Loop D and the surrounding regions of 23S rRNA of the two structures were aligned using PyMOL. The region between helices 41 and 42 is colored cyan; the loop that caps helix 39 is colored blue, and helix 89 is colored yellow. Residues in 23S rRNA that are significantly changed are colored red (pre-translocation) or green (post-translocation). Contacts between 23S rRNA and loop D nucleotides are shown for (B) C_{88}, (C) C_{91}, and (D) G_{89}.

bond of A_{90} abolishes the closing base pair of this GNRA tetraloop, and there is a lateral movement of C_{88} by more than 5 Å (relative to N4). These changes alter the path of the backbone through the loop.

Because the pre- and post-translocation ribosomes exhibit the greatest difference in the structure of loop D, we have examined these two structures more carefully. Loop D is embedded in a region that represents a confluence of domain II of 23S rRNA, which includes the GAC, and domain V, which contains the PTC (Figure 10A). Three segments of 23S rRNA are proximal to loop D: (1) the loop of helix 39 (H39), (2) a structured region that joins helices 41 and 42 from domain II, and (3) helix 89 (H89), one of the helices comprising the PTC of domain V. In addition to the changes in the position of bases A_{90} and C_{88} in 5S rRNA, the loop itself is shifted relative to the surrounding segments of 23S rRNA. This translational movement probably accounts for the ability of *E. coli* U_{89} to cross-link to residues in domains II and V.[39] The orientations of two noncontiguous bases in 23S rRNA, U_{958} and U_{1026}, also change between the two structures. The former has rotated approximately 90° around its glycosidic bond, and the latter base is shifted by 2.8 Å (relative to O4).

A search for contacts identified three possible interactions between loop D and 23S rRNA. C_{88}, which exhibits the largest movement in loop D, makes the greatest contact with 23S rRNA. In the pretranslocation ribosome, C_{88} makes potential hydrogen bonds through N4 to O3′ of nucleotide 1027 and through OP1 to O2′ of nucleotide 1026; in addition, the ribose of C_{88} is stacked on the base of U_{1026} (Figure 10B). The distance between C_{88} and this segment of 23S rRNA increases by more than 1 Å in the post-translocation structure, eliminating all these contacts. The loss of the stacking interaction between C_{88} and U_{1026} can account for the markedly different orientation of the latter residue in the two structures.

Cross-linking and mutagenesis studies have demonstrated the proximity of loop D to the 960 loop that caps helix 39 in 23S rRNA.[39,42,72] A potential (water-mediated) hydrogen bond between C_{91} (OP1) and U_{958} (O2) is found in both ribosome structures. C_{91} is in the first Watson−Crick base pair flanking loop D, and its conformation is not appreciably influenced by the changes at A_{90}; rather, its position is changed by the lateral shift of loop D. Contact between C_{91} and U_{958} is maintained by a substantial rotation (approximately 90°) of the uracil that compensates for the movement of loop D (Figure 10C). The difference in the distance between the putative hydrogen bond partners is only ~0.1 Å in the two structures, indicating coordinated changes occur in the structures of the two RNAs to maintain contact before, after, and, presumably, during translocation.

A third contact is possible between N2 of G_{89} and OP1 of G_{2487}, which is located in helix 89 in the peptidyl transferase ring (Figure 10D). This interaction is only possible in the post-translocation ribosome; the distance between these two atoms is nearly 2 Å greater in the pretranslocation ribosome. This change can be attributed mostly to the lateral movement of loop D, because the orientation of guanine 89 does not change appreciably between the two structures, nor does the position or conformation of helix 89.

The structural changes of loop D apparently result from the disruption of the $G_{87}\cdot A_{90}$ base pair, yet neither of these nucleotides appears to make contact with 23S rRNA. Loop D is a member of the familiar GNRA tertaloop family that occurs frequently in rRNA.[73] These tetraloops are characterized by a sheared *anti-anti* G·A base pair between the first and last nucleotides of the loop that contributes significantly to the stability of the structure. However, the sheared base pair in the pretranslocation ribosome appears to be compromised, having only one, rather than two, hydrogen bond between the bases. The hydrogen bond distance from G_{87} N2 to A_{90} N7 is 3.86 Å, well within the range (2.41−4.18 Å) measured for different GNRA tetraloops by NMR.[74] However, the distance from G_{87} N3 to A_{90} N6 of 5.37 Å is outside the observed range of 2.5−5.08 Å, indicating that a hydrogen bond between these latter positions is unlikely. Thus, the atypical weak interaction between these nucleotides likely explains how this base pair can be exploited and used to change the structure of the loop and, consequently, its interaction with surrounding nucleotides in 23S rRNA.

Another feature of the canonical GNRA tetraloop is the exposure of the nucleotide following the turning phosphate. This nucleotide is not involved in any internal hydrogen bonds and, thus, is the position in the tetraloop most likely to participate in tertiary interactions.[74] This is exactly what is observed in the pretranslocation ribosome where C_{88} makes two hydrogen bonds to 23S rRNA as well as a stacking interaction with U_{1026}, all of which are lost in the post-translocation ribosome.

The structural studies presented here not only refine the contact site for eukaryotic ribosomal protein L5 on 5S rRNA but also identify sites of structural changes in the RNA that are of potential functional significance. In particular, the arm of 5S rRNA comprised of loop D, helix IV, and loop E has dynamic features consistent with a role in transmitting information from one site in the large subunit to another. This raises the question of whether L5 induces a conformation in this region of the RNA that is needed for its putative relay activity. Protein-induced deformation of RNA used to promote function is seen elsewhere in the ribosome, most notably the distortion of A-site tRNA that creates a communication pathway between the decoding center in the small subunit and the GAC of the large subunit.[66,71,75−77]

■ ASSOCIATED CONTENT

Supporting Information. List of potential contacts between *H. marismortui* L5 and L18 and 5S rRNA. This material is available free of charge via the Internet at http://pubs.acs.org.

■ AUTHOR INFORMATION

Corresponding Author

*Phone: (574) 631-6042. Fax: (574) 631-6652. E-mail: huber.1@nd.edu.

Notes

[a]Nucleotide positions refer to *Xenopus* 5S rRNA unless noted otherwise.

Funding Sources

This work was supported by Grant GM38200 from the National Institutes of Health.

■ ACKNOWLEDGMENT

We are especially grateful to Jason P. Rife for advice and help with analyzing RNA structures. We are indebted to Yuen-Ling Chan for several helpful discussions, to Erica Duguid for the CONTACT/ACT analysis of intersubunit contacts between *H. marismortui* 5S rRNA and L18 and L5, and to Brian Wilson for help with PyMOL. We thank Rita Egendoerfer for the preparation of Figure 3.

■ ABBREVIATIONS

TFIIIA, transcription factor IIIA; MBP, maltose binding protein; fL5, maltose binding protein−L5 fusion protein; RNP, ribonucleoprotein.

■ REFERENCES

(1) Deshmukh, M., Tsay, Y. F., Paulovich, A. G., and Woolford, J. L., Jr. (1993)Yeast ribosomal protein L1 is required for the stability of newly synthesized 5S rRNA and the assembly of 60S ribosomal subunits. *Mol. Cell. Biol. 13*, 2835–2845.

(2) Steitz, J. A., Berg, C., Hendrick, J. P., La Branche-Chabot, H., Metspalu, A., Rinke, J., and Yario, T. (1988)A 5S rRNA/L5 complex is a precursor to ribosome assembly in mammalian cells. *J. Cell Biol. 106*, 545–556.

(3) Zhang, J., Harnpicharnchai, P., Jakovljevic, J., Tang, L., Guo, Y., Oeffinger, M., Rout, M. P., Hiley, S. L., Hughes, T., and Woolford, J. L., Jr. (2007)Assembly factors Rpf2 and Rrs1 recruit 5S rRNA and ribosomal proteins rpL5 and rpL11 into nascent ribosomes. *Genes Dev. 21*, 2580–2592.

(4) Wormington, W. M. (1989)Developmental expression and 5S rRNA-binding activity of *Xenopus laevis* ribosomal protein L5. *Mol. Cell. Biol. 9*, 5281–5288.

(5) Honda, B. M., and Roeder, R. G. (1980)Association of a 5S gene transcription factor with 5S RNA and altered levels of the factor during cell differentiation. *Cell 22*, 119–126.

(6) Joho, K. E., Darby, M. K., Crowford, E. T., and Brown, D. D. (1990)A finger protein structurally similar to TFIIIA that binds exclusively to 5S RNA in *Xenopus*. *Cell 61*, 293–300.

(7) Pelham, H. R. B., and Brown, D. D. (1980)A specific transcription factor that can bind either the 5S RNA gene or 5S RNA. *Proc. Natl. Acad. Sci. U.S.A. 77*, 4170–4174.

(8) Picard, B., le Maire, M., Wegnez, M., and Denis, H. (1980) Biochemical research on oogenesis. Composition of the 42S storage particles of *Xenopus laevis* oocytes. *Eur. J. Biochem. 109*, 359–368.

(9) Allison, L. A., Romaniuk, P. J., and Bakken, A. H. (1991)RNA-protein interactions of stored 5S RNA with TFIIIA and ribosomal protein L5 during *Xenopus* oogenesis. *Dev. Biol. 144*, 129–144.

(10) Claussen, M., Rudt, F., and Pieler, T. (1999)Functional modules in ribosomal protein L5 for ribonucleoprotein complex formation and nucleocytoplasmic transport. *J. Biol. Chem. 274*, 33951–33958.

(11) Murdoch, K. J., and Allison, L. A. (1996)A role for ribosomal protein L5 in the nuclear import of 5S rRNA in *Xenopus* oocytes. *Exp. Cell Res. 227*, 332–343.

(12) North, M. T., and Allison, L. A. (1998)Nucleolar targeting of 5S RNA in *Xenopus laevis* oocytes: Somatic-type nucleotide substitutions enhance nucleolar localization. *J. Cell. Biochem. 69*, 490–505.

(13) Rudt, F., and Pieler, T. (1996)Cytoplasmic retention and nuclear import of 5S ribosomal RNA containing RNPs. *EMBO J. 15*, 1383–1391.

(14) Rudt, F., and Pieler, T. (2001)Cytosolic import factor- and Ran-independent nuclear transport of ribosomal protein L5. *Eur. J. Cell Biol. 80*, 661–668.

(15) Baudin, F., and Romaniuk, P. J. (1989)A difference in the importance of bulged nucleotides and their parent base pairs in the binding of transcription factor IIIA to *Xenopus* 5S RNA genes. *Nucleic Acids Res. 17*, 2043–2056.

(16) Baudin, F., Romaniuk, P. J., Romby, P., Brunel, C., Westhof, E., Ehresmann, B., and Ehresmann, C. (1991)Involvement of "Hinge" nucleotides of *Xenopus laevis* 5S rRNA in the RNA structural organization and in the binding of transcription factor TFIIIA. *J. Mol. Biol. 218*, 69–81.

(17) Bogenhagen, D. F., and Sands, M. S. (1992)Binding of TFIIIA to Derivatives of 5S RNA Containing Sequence Substitutions or Deletions Defines a Minimal TFIIIa Binding Site. *Nucleic Acids Res. 20*, 2639–2645.

(18) Huber, P. W., and Wool, I. G. (1986)Identification of the binding site on 5S rRNA for the transcription factor IIIA: Proposed structure of a common binding site on 5S rRNA and on the gene. *Proc. Natl. Acad. Sci. U.S.A. 83*, 1593–1597.

(19) McBryant, S. J., Veldhoen, N., Gedulin, B., Leresche, A., Foster, M. P., Wright, P. E., Romaniuk, P. J., and Gottesfeld, J. M. (1995) Interaction of the RNA binding fingers of *Xenopus* transcription factor IIIA with specific regions of 5S ribosomal RNA. *J. Mol. Biol. 248*, 44–57.

(20) Rawlings, S. L., Matt, G. D., and Huber, P. W. (1996)Analysis of the binding of *Xenopus* transcription factor IIIA to oocyte 5S rRNA and to the 5S rRNA gene. *J. Biol. Chem. 271*, 869–877.

(21) Romaniuk, P. J. (1985)Characterization of the RNA Binding Properties of Transcription Factor IIIA of *Xenopus laevis* oocytes. *Nucleic Acids Res. 13*, 5369–5387.

(22) Romaniuk, P. J. (1989)The Role of Highly Conserved Single-Stranded Nucleotides of *Xenopus* 5S RNA in the Binding of Transcription Factor IIIA. *Biochemistry 28*, 1388–1395.

(23) Romaniuk, P. J., Stevenson, I. L. d., and Adriana, W. H.-H. (1987)Defining the Binding Site of *Xenopus* Transcription Factor IIIA on 5S RNA Using Truncated and Chimeric 5S RNA Molecules. *Nucleic Acids Res. 15*, 2737–2755.

(24) Sands, M. S., and Bogenhagen, D. F. (1991)The Carboxyterminal Zinc Fingers of TFIIIA Interact with the Tip of Helix V of 5S RNA in the 7S Ribonucleoprotein Particle. *Nucleic Acids Res. 19*, 1791–1796.

(25) You, Q., and Romaniuk, P. J. (1990)The effects of disrupting 5S RNA helical structures on the binding of *Xenopus* transcription factor IIIA. *Nucleic Acids Res. 18*, 5055–5062.

(26) Theunissen, O., Rudt, F., and Pieler, T. (1998)Structural determinants in 5S RNA and TFIIIA for 7S RNP formation. *Eur. J. Biochem. 258*, 758–767.

(27) Andersen, J., and Delihas, N. (1986)Characterization of RNA-protein interactions in 7S ribonucleoprotein particles from *Xenopus laevis* oocytes. *J. Biol. Chem. 261*, 2912–2917.

(28) Pieler, T., and Erdmann, V. A. (1983)Isolation and Characterization of a 7S RNP Particle from Mature *Xenopus laevis* Oocytes. *FEBS Lett. 157*, 283–287.

(29) Darsillo, P., and Huber, P. W. (1991)The use of chemical nucleases to analyze RNA-protein interactions: The TFIIIA-5S rRNA complex. *J. Biol. Chem. 266*, 21075–21082.

(30) Aoyama, K., Tanaka, T., Hidaka, S., and Ishikawa, K. (1984) Binding sites of rat liver 5S RNA to ribosomal protein L5. *J. Biochem. 95*, 1179–1186.

(31) Gross, B., Welfle, H., and Bielka, H. (1985)Protein-RNA interaction in the rat liver 5S rRNA-protein L5 complex studied by digestion with ribonucleases. *Nucleic Acids Res. 13*, 2325–2335.

(32) Huber, P. W., and Wool, I. G. (1986)Use of the cytotoxic nuclease α-sarcin to identify the binding site on eukaryotic 5S ribosomal ribonucleic acid for the ribosomal protein L5. *J. Biol. Chem. 261*, 3002–3005.

(33) Nazar, R. N. (1979)The ribosomal protein binding site in *Saccharomyces cerevisiae* ribosomal 5S RNA. *J. Biol. Chem. 254*, 7724–7729.

(34) Nazar, R. N., and Wildeman, A. G. (1983)Three helical domains form a protein binding site in the 5S RNA-protein complex from eukaryotic ribosomes. *Nucleic Acids Res. 11*, 3155–3168.

(35) Scripture, J. B., and Huber, P. W. (1995)Analysis of the binding of *Xenopus* ribosomal protein L5 to oocyte 5S rRNA: The major determinants of recognition are located in helix III-loop C. *J. Biol. Chem. 270*, 27358–27365.

(36) Lu, D., Alexandra Searles, M., and Klug, A. (2003)Crystal structure of a zinc-finger-RNA complex reveals two modes of molecular recognition. *Nature 426*, 96–100.

(37) Lee, B. M., Xu, J., Clarkson, B. K., Martinez-Yamout, M. A., Dyson, H. J., Case, D. A., Gottesfeld, J. M., and Wright, P. E. (2006) Induced fit and "lock and key" recognition of 5S RNA by zinc fingers of transcription factor IIIA. *J. Mol. Biol. 357*, 275–291.

(38) Huber, P. W. (1993)Chemical nucleases: Their use in studying RNA structure and RNA-protein interactions. *FASEB J. 7*, 1367–1375.

(39) Dokudovskaya, S., Dontsova, O., Shpanchenko, O., Bogdanov, A., and Brimacombe, R. (1996)Loop IV of 5S ribosomal RNA has contacts both to domain II and to domain V of the 23S RNA. *RNA 2*, 146–152.

(40) Dontsova, O., Tishkov, V., Dokudovskaya, S., Bogdanov, A., Doring, T., Rinke-Appel, J., Thamm, S., Greuer, B., and Brimacombe, R. (1994)Stem-loop IV of 5S rRNA lies close to the peptidyltransferase center. *Proc. Natl. Acad. Sci. U.S.A. 91*, 4125–4129.

(41) Kiparisov, S., Petrov, A., Meskauskas, A., Sergiev, P. V., Dontsova, O. A., and Dinman, J. D. (2005)Structural and functional analysis of 5S rRNA in *Saccharomyces cerevisiae*. *Mol. Genet. Genomics 274*, 235–247.

(42) Sergiev, P. V., Bogdanov, A. A., Dahlberg, A. E., and Dontsova, O. (2000)Mutations at position A960 of *E. coli* 23S ribosomal RNA influence the structure of 5S ribosomal RNA and the peptidyltransferase region of 23S ribosomal RNA. *J. Mol. Biol. 299*, 379–389.

(43) Smith, M. W., Meskauskas, A., Wang, P., Sergiev, P. V., and Dinman, J. D. (2001)Saturation mutagenesis of 5S rRNA in *Saccharomyces cerevisiae*. *Mol. Cell. Biol. 21*, 8264–8275.

(44) Schatz, D., Leberman, R., and Eckstein, F. (1991)Interaction of *Escherichia coli* $tRNA^{Ser}$ with its cognate aminoacyl-tRNA synthetase as determined by footprinting with phosphorothioate-containing tRNA transcripts. *Proc. Natl. Acad. Sci. U.S.A. 88*, 6132–6136.

(45) Project, C. C. (1994)The CCP4 suite: Programs for protein crystallography. *Acta Crystallogr. D50*, 760–763.

(46) Wool, I. G., Gluck, A., and Endo, Y. (1992)Ribotoxin recognition of ribosomal RNA and a proposal for the mechanism of translocation. *Trends Biochem. Sci. 17*, 266–269.

(47) Endo, Y., Huber, P. W., and Wool, I. G. (1983)The ribonuclease activity of the cytotoxin α-sarcin. The characteristics of the enzymatic activity of α-sarcin with ribosomes and ribonucleic acids as substrates. *J. Biol. Chem. 258*, 2662–2667.

(48) Huber, P. W., and Wool, I. G. (1988)Use of α-sarcin to analyze ribosomal RNA-protein interactions. *Methods Enzymol. 164*, 468–475.

(49) Tullius, T. D., Dombroski, B. A., Churchill, M. E., and Kam, L. (1987)Hydroxyl radical footprinting: A high-resolution method for mapping protein-DNA contacts. *Methods Enzymol. 155*, 537–558.

(50) Balasubramanian, B., Pogozelski, W. K., and Tullius, T. D. (1998)DNA strand breaking by the hydroxyl radical is governed by the accessible surface areas of the hydrogen atoms of the DNA backbone. *Proc. Natl. Acad. Sci. U.S.A. 95*, 9738–9743.

(51) Gish, G., and Eckstein, F. (1988)DNA and RNA sequence determination based on phosphorothioate chemistry. *Science 240*, 1520–1522.

(52) DiNitto, J. P., and Huber, P. W. (2003)Mutual induced fit binding of *Xenopus* ribosomal protein L5 to 5S rRNA. *J. Mol. Biol. 330*, 979–992.

(53) Hayes, J. J., and Tullius, T. D. (1989)The missing nucleoside experiment: A new technique to study recognition of DNA by protein. *Biochemistry 28*, 9521–9527.

(54) Ben-Shem, A., Jenner, L., Yusupova, G., and Yusupov, M. (2010) Crystal structure of the eukaryotic ribosome. *Science 330*, 1203–1209.

(55) Chandramouli, P., Topf, M., Menetret, J. F., Eswar, N., Cannone, J. J., Gutell, R. R., Sali, A., and Akey, C. W. (2008)Structure of the mammalian 80S ribosome at 8.7 Å resolution. *Structure 16*, 535–548.

(56) Ban, N., Nissen, P., Hansen, J., Moore, P. B., and Steitz, T. A. (2000)The complete atomic structure of the large ribosomal subunit at 2.4 Å resolution. *Science 289*, 905–920.

(57) Klein, D. J., Moore, P. B., and Steitz, T. A. (2004)The roles of ribosomal proteins in the structure assembly, and evolution of the large ribosomal subunit. *J. Mol. Biol. 340*, 141–177.

(58) Neely, L. S., Lee, B. M., Xu, J., Wright, P. E., and Gottesfeld, J. M. (1999)Identification of a minimal domain of 5S ribosomal RNA sufficient for high affinity interactions with the RNA-specific zinc fingers of transcription factor IIIA. *J. Mol. Biol. 291*, 549–560.

(59) Searles, M. A., Lu, D., and Klug, A. (2000)The role of the central zinc fingers of transcription factor IIIA in binding to 5S RNA. *J. Mol. Biol. 301*, 47–60.

(60) Spahn, C. M., Beckmann, R., Eswar, N., Penczek, P. A., Sali, A., Blobel, G., and Frank, J. (2001)Structure of the 80S ribosome from *Saccharomyces cerevisiae*: tRNA-ribosome and subunit-subunit interactions. *Cell 107*, 373–386.

(61) Spierer, P., Bogdanov, A. A., and Zimmermann, R. A. (1978) Parameters for the interaction of ribosomal proteins L5, L18, and L25 with 5S RNA from *Escherichia coli*. *Biochemistry 17*, 5394–5398.

(62) Spierer, P., and Zimmermann, R. A. (1978)Stoichiometry, cooperativity, and stability of interactions between 5S RNA and proteins L5, L18, and L25 from the 50S ribosomal subunit of *Escherichia coli*. *Biochemistry 17*, 2474–2479.

(63) Smirnov, A. V., Entelis, N. S., Krasheninnikov, I. A., Martin, R., and Tarassov, I. A. (2008)Specific features of 5S rRNA structure: Its interactions with macromolecules and possible functions. *Biochemistry (Moscow, Russ. Fed.) 73*, 1418–1437.

(64) Tullius, T. D., and Greenbaum, J. A. (2005)Mapping nucleic acid structure by hydroxyl radical cleavage. *Curr. Opin. Chem. Biol. 9*, 127–134.

(65) Nissen, P., Ippolito, J. A., Ban, N., Moore, P. B., and Steitz, T. A. (2001)RNA tertiary interactions in the large ribosomal subunit: The A-minor motif. *Proc. Natl. Acad. Sci. U.S.A. 98*, 4899–4903.

(66) Stark, H., Orlova, E. V., Rinke-Appel, J., Junke, N., Mueller, F., Rodnina, M., Wintermeyer, W., Brimacombe, R., and van Heel, M. (1997)Arrangement of tRNAs in pre- and posttranslocational ribosomes revealed by electron cryomicroscopy. *Cell 88*, 19–28.

(67) Komoda, T., Sato, N. S., Phelps, S. S., Namba, N., Joseph, S., and Suzuki, T. (2006)The A-site finger in 23S rRNA acts as a functional attenuator for translocation. *J. Biol. Chem. 281*, 32303–32309.

(68) Meskauskas, A., and Dinman, J. D. (2001)Ribosomal protein L5 helps anchor peptidyl-tRNA to the P-site in *Saccharomyces cerevisiae*. *RNA 7*, 1084–1096.

(69) Selmer, M., Dunham, C. M., Murphy, F. V. t., Weixlbaumer, A., Petry, S., Kelley, A. C., Weir, J. R., and Ramakrishnan, V. (2006) Structure of the 70S ribosome complexed with mRNA and tRNA. *Science 313*, 1935–1942.

(70) Voorhees, R. M., Weixlbaumer, A., Loakes, D., Kelley, A. C., and Ramakrishnan, V. (2009)Insights into substrate stabilization from snapshots of the peptidyl transferase center of the intact 70S ribosome. *Nat. Struct. Mol. Biol. 16*, 528–533.

(71) Schmeing, T. M., Voorhees, R. M., Kelley, A. C., Gao, Y. G., Murphy, F. V. t., Weir, J. R., and Ramakrishnan, V. (2009)The crystal structure of the ribosome bound to EF-Tu and aminoacyl-tRNA. *Science 326*, 688–694.

(72) Sergiev, P., Dokudovskaya, S., Romanova, E., Topin, A., Bogdanov, A., Brimacombe, R., and Dontsova, O. (1998)The environment of 5S rRNA in the ribosome: Cross-links to the GTPase-associated area of 23S rRNA. *Nucleic Acids Res. 26*, 2519–2525.

(73) Antao, V. P., Lai, S. Y., and Tinoco, I., Jr. (1991)A thermodynamic study of unusually stable RNA and DNA hairpins. *Nucleic Acids Res. 19*, 5901–5905.

(74) Jucker, F. M., Heus, H. A., Yip, P. F., Moors, E. H., and Pardi, A. (1996)A network of heterogeneous hydrogen bonds in GNRA tetraloops. *J. Mol. Biol. 264*, 968–980.

(75) Schuette, J. C., Murphy, F. V. t., Kelley, A. C., Weir, J. R., Giesebrecht, J., Connell, S. R., Loerke, J., Mielke, T., Zhang, W., Penczek, P. A., Ramakrishnan, V., and Spahn, C. M. (2009)GTPase activation of elongation factor EF-Tu by the ribosome during decoding. *EMBO J. 28*, 755–765.

(76) Valle, M., Sengupta, J., Swami, N. K., Grassucci, R. A., Burkhardt, N., Nierhaus, K. H., Agrawal, R. K., and Frank, J. (2002)Cryo-EM reveals an active role for aminoacyl-tRNA in the accommodation process. *EMBO J. 21*, 3557–3567.

(77) Villa, E., Sengupta, J., Trabuco, L. G., LeBarron, J., Baxter, W. T., Shaikh, T. R., Grassucci, R. A., Nissen, P., Ehrenberg, M., Schulten, K., and Frank, J. (2009)Ribosome-induced changes in elongation factor Tu conformation control GTP hydrolysis. *Proc. Natl. Acad. Sci. U.S.A. 106*, 1063–1068.